Original Article

miR-204 suppresses cancer stemness and enhances osimertinib sensitivity in non-small cell lung cancer by targeting CD44

Shang-Gin Wu,[1,2] Tzu-Hua Chang,[2] Meng-Feng Tsai,[3] Yi-Nan Liu,[2] Yen-Lin Huang,[4,5] Chia-Lang Hsu,[6] Han-Nian Jheng,[2] and Jin-Yuan Shih[2,7]

[1]Department of Internal Medicine, National Taiwan University Cancer Center, National Taiwan University, Taipei 10672, Taiwan; [2]Department of Internal Medicine, National Taiwan University Hospital, National Taiwan University, Taipei 10002, Taiwan; [3]Department of Biomedical Sciences, Da-Yeh University, Changhua 51591, Taiwan; [4]Department of Pathology, National Taiwan University Cancer Center, National Taiwan University, Taipei 10672, Taiwan; [5]Department of Pathology, National Taiwan University Hospital, National Taiwan University, Taipei 10002, Taiwan; [6]Department of Medical Research, National Taiwan University Hospital, National Taiwan University, Taipei 10002, Taiwan; [7]Graduate Institute of Clinical Medicine, College of Medicine, National Taiwan University, Taipei 10002, Taiwan

Osimertinib is an effective treatment option for patients with advanced non-small cell lung cancer (NSCLC) with *EGFR* activation or T790M resistance mutations; however, acquired resistance to osimertinib can still develop. This study explored novel miRNA–mRNA regulatory mechanisms that contribute to osimertinib resistance in lung cancer. We found that miR-204 expression in osimertinib-resistant lung cancer cells was markedly reduced compared to that in osimertinib-sensitive parental cells. miR-204 expression levels in cancer cells isolated from treatment-naive pleural effusions were significantly higher than those in cells with acquired resistance to osimertinib. miR-204 enhanced the sensitivity of lung cancer cells to osimertinib and suppressed spheroid formation, migration, and invasion of lung cancer cells. Increased miR-204 expression in osimertinib-resistant cells reversed resistance to osimertinib and enhanced osimertinib-induced apoptosis by upregulating BIM expression levels and activating caspases. Restoration of *CD44* (the direct downstream target gene of miR-204) expression reversed the effects of miR-204 on osimertinib sensitivity, recovered cancer stem cell and mesenchymal markers, and suppressed E-cadherin expression. The study demonstrates that miR-204 reduced cancer stemness and epithelial-to-mesenchymal transition, thus overcoming osimertinib resistance in lung cancer by inhibiting the CD44 signaling pathway.

INTRODUCTION

Lung cancer remains the leading cause of cancer-related death worldwide. In most countries, the 5-year survival rate of lung cancer patients is only 10%–20%.[1] Histologically, non-small cell lung cancer (NSCLC) accounts for approximately 85% of lung cancer cases.[2] Traditional treatment options for NSCLC include surgical resection, radiation therapy, and platinum-based chemotherapy.[3] However, these treatment options are often associated with limited efficacy and poor prognoses. Currently, molecular-targeted therapies are an emerging treatment option for patients with NSCLC. The epidermal growth factor receptor (*EGFR*) is one of the most established molecular targets in NSCLC. Aberrant expression and constitutive activation of the EGFR signaling pathway are involved in the development and progression of many human cancers, including NSCLC.[4] Approximately 40%–50% of nonsquamous NSCLC patients in Asia and 10%–20% of patients in Western countries have tumors harboring *EGFR* somatic activating mutations (e.g., exon 19 deletions, L858R point mutation).[5,6] Patients with *EGFR*-mutant NSCLC respond favorably to EGFR-tyrosine kinase inhibitors (TKIs).[7]

Most NSCLC patients who were treated with first- or second-generation EGFR-TKIs eventually developed acquired resistance after 8–14 months, and approximately 50%–60% of these patients had an acquired resistance mutation, T790M.[8,9] In 2015, osimertinib, a third-generation EGFR-TKI, was confirmed to be effective for treating NSCLC patients with acquired *EGFR* T790M mutation.[10] After 3 years, osimertinib was approved as a first-line therapy for patients with advanced *EGFR* mutant NSCLC, irrespective of the T790M mutation status.[11] However, despite the initial dramatic response to osimertinib, patients invariably develop acquired resistance.[12] Novel treatment strategies are necessary to conquer the acquired resistance to osimertinib. Several osimertinib resistance mechanisms have been identified, including *EGFR*-dependent and *EGFR*-independent mechanisms. *EGFR* C797S mutation and *EGFR* amplification are *EGFR*-dependent mechanisms of osimertinib resistance.[12,13] *EGFR*-independent mechanisms of osimertinib resistance have been demonstrated, including *MET* amplification, *HER2* amplification,

and *PIK3CA* gene mutations.[12,14] In addition, nearly 50% of NSCLC patients acquired resistance to osimertinib for reasons that remain unclear. Further investigations are important to reveal the potential novel mechanisms of acquired resistance to osimertinib.

MicroRNAs (miRNAs) are small noncoding RNA molecules harboring approximately 22 nt in length, which negatively regulate gene expression by directly targeting mRNAs.[15] They play crucial roles in various pathophysiological functions, including cell differentiation, embryonic development, metabolism, and intercellular communication.[16] Accumulating evidence suggests that the aberrant expression of miRNAs affects tumor initiation, metastasis, and progression.[15–17] miRNAs are also involved in the resistance to chemotherapy or EGFR-TKIs in lung cancer.[18–20] Exosomal miRNAs, miR-184 and miR-3913-5p, have been reported as potential biomarkers for osimertinib resistance in patients with NSCLC.[21] Exosome-derived miR-210 is associated with osimertinib resistance and enhanced epithelial-to-mesenchymal transition (EMT) in HCC827 cells, which has an exon 19 deletion of *EGFR*.[22] Our previous study indicated that EGFR-TKI-resistant cells expressed a lower level of miR-146b-5p. Forced expression of miR-146b-5p restored osimertinib sensitivity in osimertinib-resistant primary NSCLC cancer cells (PE2988 and PE3479).[19]

miR-204 plays important roles in many biological functions, including osteogenesis, adipogenesis, lens morphogenesis, and multiple pathological processes.[23] miR-204, highly expressed in the retinal pigment epithelium layer, is a major regulator of ocular development and normal maintenance. miR-204 is essential for normal photoreceptor cell differentiation and homeostasis.[24,25] Moreover, high endogenous miR-204 expression has been observed more in the human kidney compared to other organs.[26] Downregulated miR-204 expression has been observed in progressive chronic kidney disease.[27,28] In addition, miR-204 has been identified as a tumor suppressor in various human cancers.[29–34] Breast cancer patients with low miR-204 expression have shorter overall and disease-free survival.[32] Restoring miR-204 expression repressed proliferation and invasion and promoted sensitivity to chemotherapeutic agents in colorectal cancer cells.[30] Furthermore, lower miR-204 expression levels in the plasma were significantly correlated with poor prognosis in NSCLC patients.[31] However, the role of miR-204 in osimertinib resistance remains unclear.

This study aimed to explore novel miRNAs and downstream regulatory mechanisms that contribute to osimertinib resistance in lung cancer. We demonstrate that miR-204 promotes osimertinib sensitivity in lung cancer by targeting *CD44*. These findings provide novel perceptions into the functions of miR-204 and *CD44* in lung cancer and the molecular mechanisms underlying osimertinib resistance. This study lays the groundwork for restoring osimertinib sensitivity in patients who have developed treatment resistance, which could enhance clinical outcomes and reduce lung cancer mortality.

RESULTS

miR-204 expression was significantly decreased in osimertinib-resistant cells

To explore potential miRNA candidates associated with osimertinib treatment response, different lung cancer cell lines, including osimertinib-sensitive and osimertinib-resistant cells, were collected. Osimertinib-resistant cells (HCC827/gef [gefitinib], PC9/gef, H1975/AZD15, and H1975/AZD18) were selected from the parental cells (HCC827, PC9, and H1975) after continuous exposure to EGFR-TKIs, gefitinib, or osimertinib, according to a dose-escalation procedure. HCC827, PC9, and H1975 cells were sensitive to osimertinib, with less than 0.02 μM of half-maximal inhibitory concentration (IC_{50}) after treatment with osimertinib for 96 h, whereas HCC827/gef, PC9/gef, H1975/AZD15, and H1975/AZD18 were resistant to osimertinib, with IC_{50} values greater than 1 μM (Figure 1A). All of the osimertinib-resistant cells exhibited at least a 100-fold greater IC_{50} than did the parental cells. The *EGFR* mutation status and IC_{50} values of osimertinib in the human lung cancer cell lines used in this study are shown in Figure 1A and Table S1.

We compared the expression profiles of miRNA in osimertinib-sensitive HCC827 with those in osimertinib-resistant HCC827/gef cells using the TaqMan Array Human MicroRNA A+B Cards Set.[19] The expression of miR-204 in osimertinib-sensitive HCC827 cells was higher than that in osimertinib-resistant HCC827/gef cells. To validate this finding, we detected miR-204 expression levels in osimertinib-sensitive and osimertinib-resistant cells using qRT-PCR. The results confirmed that miR-204 expression was remarkably lower in osimertinib-resistant cells (HCC827/gef: 0.38-fold, PC9/gef: 0.4-fold, H1975/AZD15: 0.28-fold, H1975/AZD18: 0.2-fold) than in parental controls (PC9, HCC827, and H1975) (Figure 1B).

miR-204 was downregulated in MPE of lung adenocarcinoma after resistance to osimertinib

A total of 157 malignant pleural effusions (MPEs) from patients with lung adenocarcinoma harboring *EGFR* mutations was collected. Among these, 105 MPEs were collected at the initial diagnosis of lung cancer before systemic treatment, whereas the other 52 MPEs were collected after the patient acquired resistance to osimertinib (26 samples) or other first-generation EGFR-TKIs (20 gefitinib and 6 erlotinib). Table S2 showed the clinical characteristics of the patients. Primary cancer cells were isolated from MPEs, and miR-204 expression levels were determined using qRT-PCR. The results indicated that the median miR-204 expression level was significantly higher in MPEs collected from treatment-naive pleural effusions than in those obtained after the acquisition of osimertinib resistance ($p = 0.03645$, by Mann-Whitney U test; Figure 1C). The results also showed that MPEs collected from patients after acquired resistance to other first-generation EGFR-TKIs had significantly lower median expression of miR-204 ($p = 0.00059$, by Mann-Whitney U test; Figure 1C).
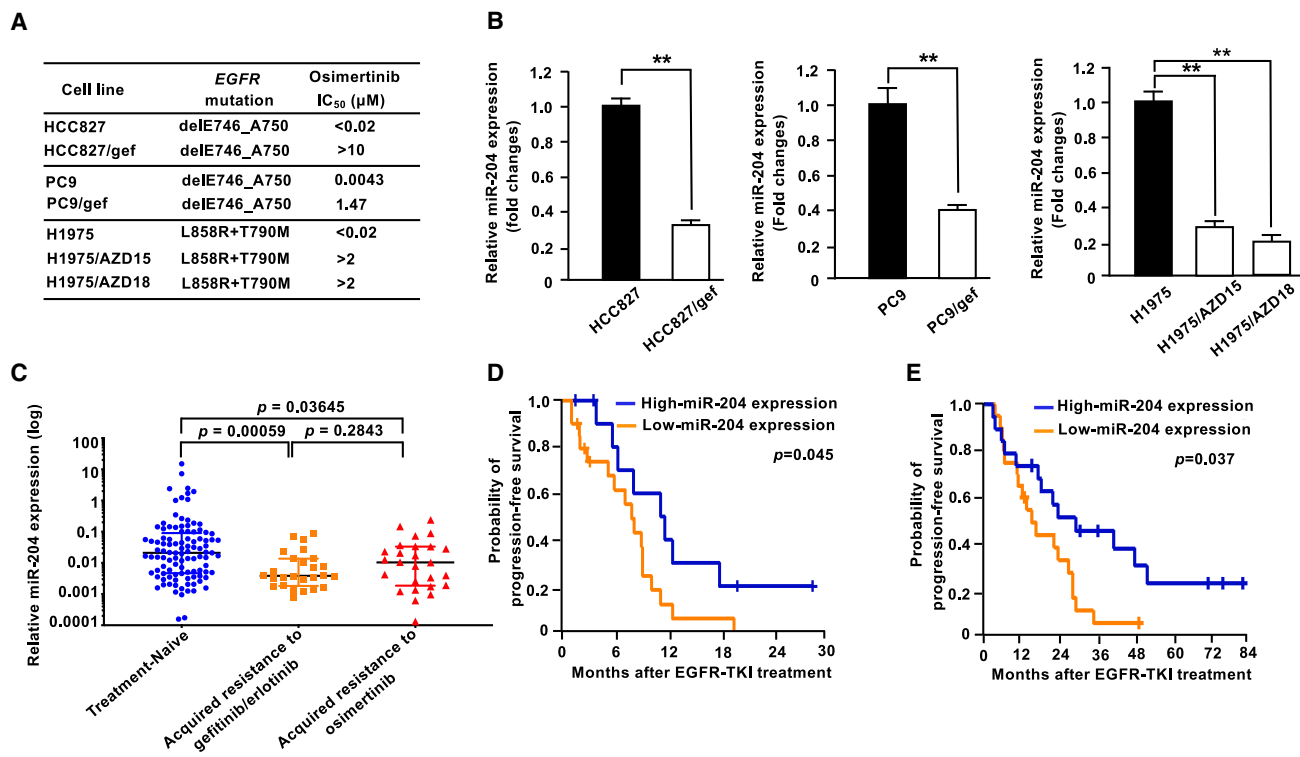
Figure 1. miR-204 expression was decreased in osimertinib-resistant lung cancer cells

(A) The *EGFR* mutation status and IC_{50} values of osimertinib in human lung cancer cell lines examined in this study are summarized. The growth inhibitory effects of osimertinib were measured using an MTT assay, as described in materials and methods. (B) qRT-PCR was performed to validate the miR-204 expression in the osimertinib-sensitive and osimertinib-resistant cell lines (**$p < 0.01$; p values were determined by Student's t test). (C) The miR-204 mRNA levels were detected in primary cancer cells isolated from 157 MPEs of lung adenocarcinoma patients using qRT-PCR. Treatment-naive lung cancer patients (n = 105); lung cancer patients with acquired resistance to osimertinib (n = 26); lung cancer patients with acquired resistance to other first-generation EGFR-TKI (gefitinib and erlotinib; n = 26). The expression level of serum miR-204 was measured by qRT-PCR, and the statistical comparison between the 2 groups by Mann-Whitney *U* test. Using qRT-PCR, the miR-204 expression levels in (D) the plasma (n = 32) and (E) the surgically resected tumor specimens (n = 39) were detected. Kaplan-Meier analysis of the relationship between miR-204 expression in plasma or tumor specimen and progression-free survival of EGFR-TKI-treated lung cancer patients.

High miR-204 level was associated with longer progression-free survival of EGFR-TKI

We next validated the impact of miR-204 on the effectiveness of EGFR-TKIs in clinical practice. We collected 32 peripheral blood samples from patients with advanced lung adenocarcinoma with *EGFR* mutations who received EGFR-TKIs as first-line single-agent treatment (28 gefitinib and 4 erlotinib). The clinical characteristics of the patients are presented in Table S3. qRT-PCR was used to measure serum miR-204 expression levels. The mean value (12.5 fmol) of miR-204 expression was used as the cutoff point to define high miR-204 expression and low miR-204 expression groups. No remarkable differences in the clinical characteristics between the high and low miR-204 expression groups were observed (Table S3). Patients with high expression of miR-204 had a longer median progression-free survival (PFS) following EGFR-TKIs treatment than those with low expression of miR-204, as shown by Kaplan-Meier survival analyses and log rank tests (11.0 versus 7.8 months; hazard ratio [HR] = 0.45; 95% confidence interval [CI] 0.21–0.98, p = 0.045; Figure 1D).

Moreover, we retrieved 39 surgically resected tumor specimens from *EGFR*-mutant lung adenocarcinoma patients who had received EGFR-TKIs as a first-line treatment after tumor recurrence. All of the surgically resected tumors had common *EGFR* mutations (24 exon 19 deletion and 15 L858R mutations) (Table S4). The median fold change (0.016) of miR-204 compared with *RNU6B* normalization in tumor specimens from 39 patients was used as the cutoff point to define the high and low miR-204 expression groups. The results also indicated that the high miR-204-expression group had a longer median PFS with EGFR-TKIs than the low miR-204-expression groups (28.5 versus 14.6 months; HR = 0.49; 95% CI 0.24–1.00, p = 0.037; Figure 1E). miR-204 expression level may be a novel biomarker for predicting the effectiveness of EGFR-TKIs in lung cancer treatment.

Suppression of miR-204 led to osimertinib resistance in osimertinib-sensitive cells

A miR-204-specific inhibitor (anti-miR-204; antisense oligonucleotides) was used to silence miR-204 expression in osimertinib-sensitive
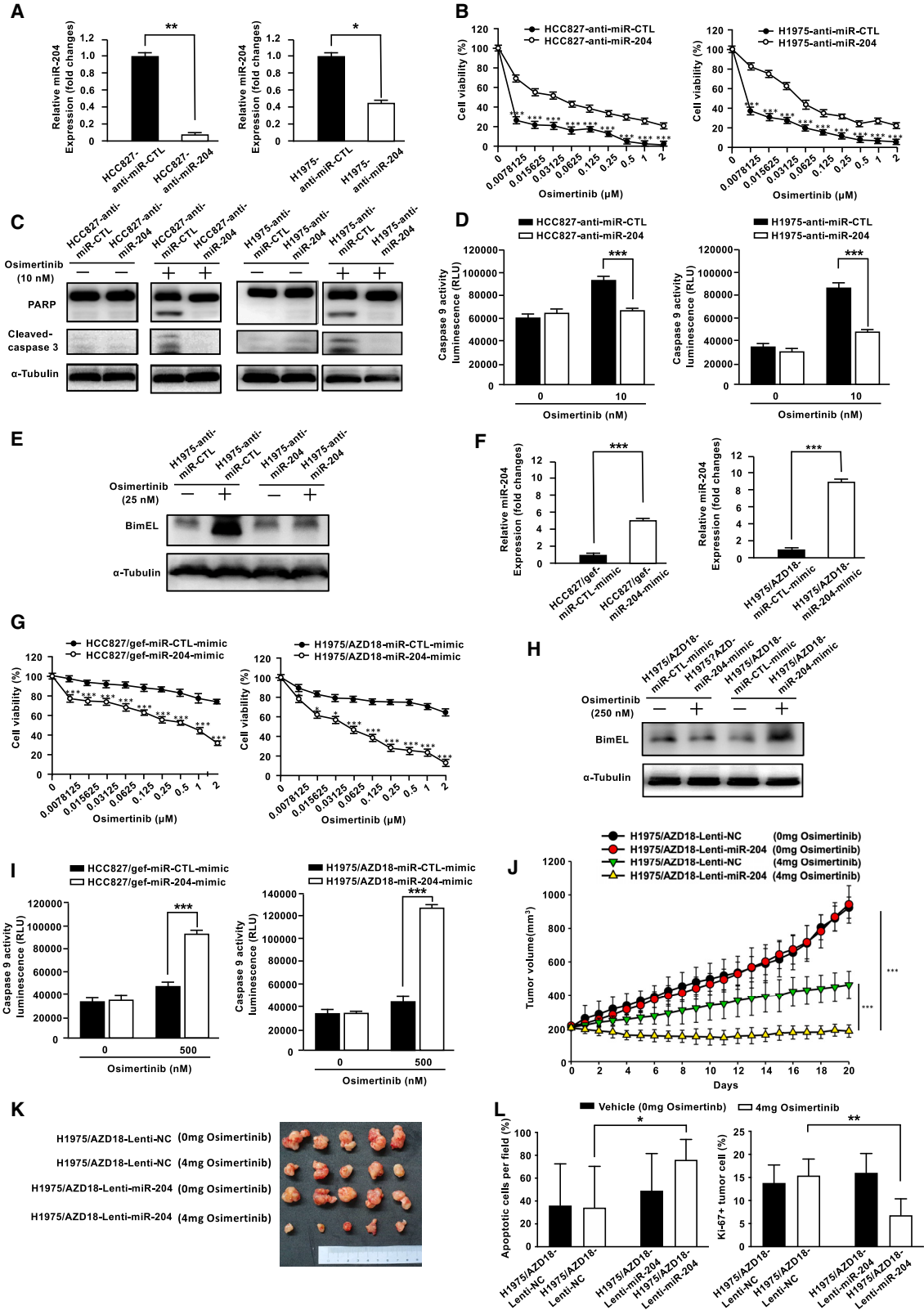
lung cancer cells (HCC827 and H1975 cells; Figure 2A). After transfection, the miR-scramble control (HCC827-anti-miR-CTL, and H1975-anti-miR-CTL) or miR-204-knockdown transfectants (HCC827-anti-miR-204 and H1975-anti-miR-204) were exposed to osimertinib, and cell viability and apoptosis markers were analyzed. Suppression of miR-204 expression by an miR-204-specific inhibitor in osimertinib-sensitive lung cancer cells conferred resistance to osimertinib (Figure 2B). Inhibition of miR-204 expression in osimertinib-sensitive lung cancer cells (HCC827 and H1975) remarkably attenuated osimertinib-induced apoptosis (poly-ADP-ribose polymerase [PARP], cleavage of caspase-3, caspase-9 activity, and B cell lymphoma 2 interacting mediator of cell death-extra long [BimEL]; Figures 2C–2E).

Increased miR-204 expression in osimertinib-resistant cells enhanced osimertinib-induced cell death

To further investigate whether the upregulation of miR-204 promoted osimertinib sensitivity in lung cancer, an miR-204-specific mimic (Thermo Fisher Scientific, Waltham, MA), a double-stranded RNA designed to mimic endogenous mature miRNA, was transiently transfected into osimertinib-resistant cells. As shown in Figure 2F, the miR-204-expression transfectants (HCC827/gef-miR-204-mimic and H1975/AZD18-miR-204-mimic) expressed higher levels of miR-204 than the control transfectants (HCC827/gef-miR-CTL-mimic and H1975/AZD18-miR-CTL-mimic). The miR-204-expression and control transfectants were exposed to osimertinib, and cell viability was analyzed using the 3-(4,5-dimethylthiazol-2-yl)-2,5-diphenyl-^{2}H-tetrazolium bromide (MTT) assay. The results showed that increased miR-204 expression in osimertinib-resistant cells enhanced the sensitivity to osimertinib (Figure 2G). The upregulation of miR-204 expression in osimertinib-resistant lung cancer cells (HCC827/gef and H1975/AZD18) promoted osimertinib-induced cell death (BimEL, and caspase 9 activity; Figures 2H and 2I).

In addition to miR-204, our previous study showed that the overexpression of miR-146b-5p enhanced osimertinib sensitivity.[19] We conducted a study to compare the effectiveness of miR-204 and miR-146b-5p on enhancing osimertinib sensitivity in osimertinib-resistant HCC827/gef cells. Forced expression of miR-204 or miR-146b-5p in osimertinib-resistant cells enhanced osimertinib sensitivity (Figure S1). The combined expression of miR-204 and miR-146b-5p

did not have a stronger effect on cell death than miR-204-mimic alone (Figure S1). This result suggested that miR-204 and miR-146-5p may have a common final pathway on osimertinib-induced cell death.

miR-204 enhanced osimertinib sensitivity *in vivo*

The effect of miR-204 on osimertinib sensitivity was determined using a tumor xenograft growth assay. The miR-204 constitutive-expressing osimertinib-resistant cells (H1975/AZD18-Lenti-miR-204; H1975/AZD18 cells transfected with Lenti-miR-204 expression construct) and negative control cells (H1975/AZD18-Lenti-NC) were injected subcutaneously into athymic nude mice. When the tumor volumes reached the start size (approximately 200 mm^3), the mice were randomized into vehicle- or osimertinib-treated groups. Mice (n = 5 in each subgroup) were dosed daily by oral gavage with vehicle or 4 mg/kg osimertinib for the duration of the treatment period. The *in vivo* xenograft studies revealed that miR-204 expression did not affect the growth of xenografts in vehicle groups (H1975/AZD18-Lenti-NC versus H1975/AZC18-Lenti-miR-204.) However, osimertinib significantly reduced tumor volume in H1975/AZD18-Lenti-miR-204 (high miR-204 expression lung cancer cells) xenografts, compared to H1975/AZD18-Lenti-NC (low miR-204 expression lung cancer cells) xenografts (Figures 2J and 2K). miR-204 expression repressed the growth of xenografts after osimertinib treatment. Consistent with *in vitro* observations, H1975/AZD18-Lenti-miR-204 xenografts were more sensitive to osimertinib treatment than were H1975/AZD18-Lenti-NC xenografts.
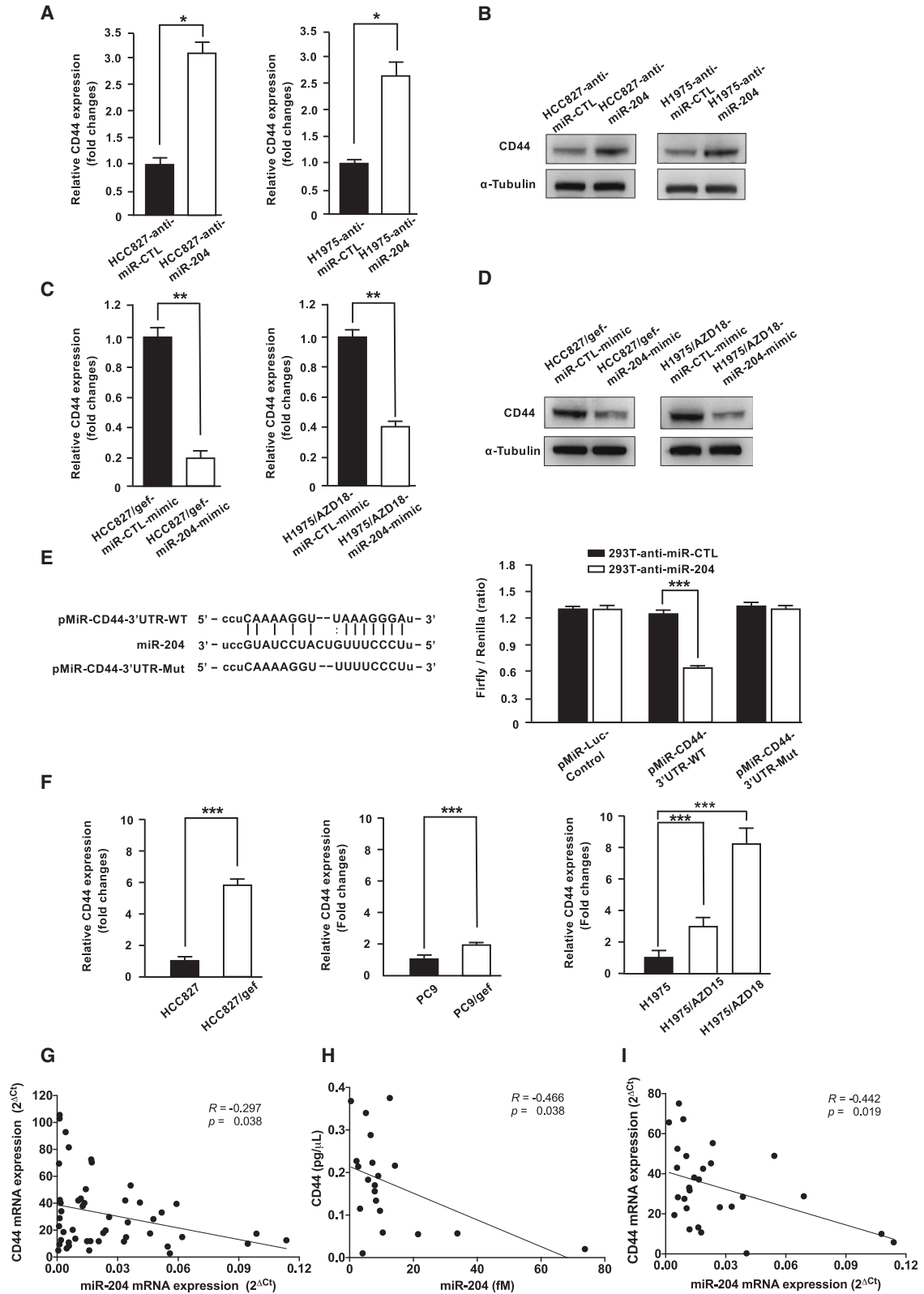
In addition, apoptotic cells in the tumor xenografts were determined using TUNEL apoptosis assays (Figure S2). After osimertinib treatment, the proportion of apoptotic cells was significantly higher in the H1975/AZD18-Lenti-miR-204 xenografts than in the H1975/AZD18-Lenti-NC xenografts (p = 0.048; Figure 2L, left). Furthermore, the proportion of Ki-67$^+$ cells was significantly lower in the H1975/AZD18-Lenti-miR-204 xenografts than in the H1975/AZD18-Lenti-NC xenografts (p = 0.005; Figures 2L, right andS2). The TUNEL apoptosis assay results also supported that miR-204 enhanced osimertinib-induced cell death in lung cancer.

CD44 was the direct downstream target gene of miR-204

To elucidate the potential mechanisms of miR-204-mediated osimertinib treatment responses in lung cancer, online prediction tools for

Figure 2. miR-204 increased the sensitivity of lung cancer cells to osimertinib
(A) The miR-204 expression level was measured by qRT-PCR in miR-204-knockdown (HCC827-anti-miR-204, H1975-anti-miR-204) and the corresponding miR-scramble control (HCC827-anti-miR-CTL, H1975-anti-miR-CTL) transfectants (*p < 0.05; **p < 0.01). (B) The cellular viability of miR-204-knockdown and control transfectants was determined following treatment with various doses of osimertinib for 96 h in MTT assays. Error bars show the SDs for n = 3 independent experiments (***p < 0.001). (C) The miR-204-knockdown and control transfectants were exposed to 10 nM of osimertinib for 24 h. Cleaved PARP and caspase-3 were assayed by western blotting. (D) Caspase-9 activity of was measured using caspase activity assay. Error bars show the SDs for n = 3 independent experiments (***p < 0.001). (E) The H1975-anti-miR-204 and H1975-anti-miR-CTL transfectants were treated with 25 nM of osimertinib for 24 h. Proapoptosis protein, BimEL, expression was determined by western blotting. (F) The expression level of miR-204 in miR-204-mimic-transfected or miR-scramble-control (miR-CTL) cells was confirmed by qRT-PCR (***p < 0.001). (G) Cell viabilities were analyzed using the MTT assay (*p < 0.05; ***p < 0.001). (H) Cells were treated with 25 nM of osimertinib for 24 h, and BimEL protein expression was determined by western blotting. (I) Caspase-9 activity was measured by a caspase activity assay system (***p < 0.001). (J) For the tumor xenograft growth assay, tumor volumes were measured every 2 days. Mice were dosed (4 mg/kg osimertinib or vehicle control) daily by oral gavage for 20 days (n = 5 in each subgroup) (***p < 0.001). (K) Images of the tumor xenografts. (L) Apoptotic cells in tumor xenografts were detected by TUNEL assay (*p < 0.05). Ki-67$^+$ cancer cells were also detected by immunohistochemical stains (**p < 0.01). p values were determined by Student's t test.

the target genes miRanda (https://cbio.mskcc.org/miRNA2003/miranda.html), miRWalk (http://mirwalk.umm.uni-heidelberg.de/), and TargetScan (http://www.targetscan.org/) were adopted. CD44, a transmembrane receptor involved in cancer stemness, aggressiveness, and drug resistance,[35] has a complementary base pairing with the seeding region of miR-204 in the 3′ UTR. qRT-PCR and western blot analysis were performed to detect CD44 expression levels in miR-204-overexpression and miR-204-knockdown lung cancer transfectants. Both the mRNA and protein expression of CD44 were substantially upregulated in miR-204-knockdown transfectants (HCC827-anti-miR-204 and H1975-anti-miR-204) (Figures 3A and 3B), and CD44 expression was repressed in miR-204-overexpression transfectants (HCC827/gef-miR-204-mimic and H1975/AZD18-miR-204-mimic) compared with the control (Figures 3C and 3D). The expression levels of miR-204 and *CD44* in lung cancer cells were negatively correlated, including in H1975, H1975/AZD15, H1975/AZD18, and two osimertinib-resistant MPE-derived cell lines (PE2988 and PE3479) (Figure S3). Directed targeting between the 3′ UTR of *CD44* and miR-204 was evaluated using a dual-luciferase reporter assay. Luciferase activity in 293T cells was significantly suppressed only when cotransfected with the wild-type (WT) 3′ UTR of *CD44* (pMIR-CD44-3′UTR-WT luciferase reporter vector) and miR-204-specific mimic, but not the binding site mutation in the 3′ UTR of *CD44* (pMIR-CD44-3′UTR-Mut luciferase reporter vector; Figure 3E). These results revealed that *CD44* is an miR-204 directed target gene in lung cancer cells. miR-204 suppressed both mRNA and protein expression levels of CD44 in lung cancer cells. To validate this finding, we evaluated *CD44* expression in osimertinib-sensitive and osimertinib-resistant cells by qRT-PCR. The results showed that CD44 expression was remarkably increased in osimertinib-resistant cells (PC9/gef, HCC827/gef, H1975/AZD15, and H1975/AZD18) compared to that in the parental controls (PC9, HCC827, and H1975; Figure 3F).

To verify the relationship between miR-204 and *CD44* expression, *CD44* mRNA expression was analyzed in tumor samples *in vivo*. A significant negative correlation was observed between miR-204 and *CD44* mRNA expression in xenografts ($R = -0.4532$; $p = 0.0448$) (Figure S4).

In addition, we analyzed *CD44* mRNA expression in 49 MPEs, 20 peripheral blood samples, and 28 surgically resected *EGFR*-mutant lung adenocarcinomas, including only samples with adequate tissue and sufficient RNA for qRT-PCR analysis. We found a significant negative correlation between miR-204 and *CD44* expression in all three sample types (MPEs: $R = -0.297$, $p = 0.038$; peripheral blood samples: $R = -0.466$, $p = 0.038$; surgically resected *EGFR*-mutant lung adenocarcinomas: $R = -0.442$, $p = 0.019$) (Figures 3G–3I). These results from cell lines and clinical samples demonstrated an inverse correlation between miR-204 and *CD44* expression.

miR-204 suppressed lung cancer cell stemness through targeting *CD44*

CD44, a cancer stem cell (CSC) marker, has been reported to play a crucial role in enriching the population and regulating the properties of lung CSCs, including cancer metastasis and drug resistance.[36–39] Thus, we speculated that miR-204 represses cancer stemness and promotes osimertinib-induced cell death in lung cancer by targeting the CD44 signaling pathway.

Cancer stemness phenotypes were validated based on the tumor spheroid formation assay and CSC marker expression (NANOG, OCT4, and SOX2). The results showed that increased tumor spheroid formation and CSC marker expression were observed in miR-204-knockdown transfectants (HCC827-anti-miR-204 and H1975-anti-miR-204; Figures 4A–4C and S8). After statistically analyzing the protein band signals, we found that the expression of stemness markers (NANOG, OCT4, and SOX2) was significantly higher in miR-204-knockdown transfectants than in control transfectants (Figure S5). However, miR-204-expression transfectants (HCC827/gef-miR-204-mimic and H1975/AZD18-miR-204-mimic) reduced tumor spheroid formation and CSC marker expression compared to control transfectants (Figures 4D–4F and S8). To confirm the effect of *CD44* on cancer stemness in lung adenocarcinoma, two *CD44*-specific-small interfering RNAs (siRNAs) (si-CD44-1 and si-CD44-2) were used to knock down *CD44* expression. Knock down *CD44* expression in HCC827/gef and H1975/AZD-18 cells reduced lung cancer cell stemness were also indicated in Figures 4G and 4H. Taken together, these results suggest that miR-204 decreases cancer stemness in lung cancer cells by targeting CD44 (Figures 3 and 4).

miR-204 attenuated lung cancer cell migration and invasion through suppression of *CD44*

In addition to tumor spheroid formation, the involvement of miR-204 in cancer migration and invasion was examined. Upregulated miR-204 expression in osimertinib-resistant cells (HCC827/gef-miR-204-mimic, and H1975/AZD 18-miR-204-mimic) remarkably inhibited tumor migration (Figure 5A) and invasion (Figure 5B). Conversely, suppression of miR-204 in osimertinib-sensitive cells (HCC827-anti-miR-204 and H1975-anti-miR-204) promoted cancer

Figure 3. CD44 was the direct target of miR-204 in lung cancer

(A and C) The CD44 mRNA expression was evaluated by using qRT-PCR (*$p < 0.05$; **$p < 0.01$). (B and D) The CD44 protein expression was detected by western blotting. (E) The miR-204 complementary binding site in the region of CD44-3′ UTR was shown. Cells were cotransfected with the pMIR-CD44-3′ UTR-WT reporter plasmid or pMIR-CD44-3′ UTR-Mut reporter, plus miR-CTL or miR-204 mimics. The luciferase activity was determined using Dual-Glo luciferase reporter assay. The relative Firefly luciferase activity was normalized to Renilla luciferase activity (***$p < 0.001$). (F) The CD44 mRNA expression was detected by using qRT-PCR in osimertinib-sensitive (HCC827, PC9, and H1975) and osimertinib-resistant cells (HCC827/gef, PC9/gef, H1975/AZD15, and H1975/AZD18) (***$p < 0.001$). p values were determined by Student's t test. Using qRT-PCR, there was a significant negative correlation between miR-204 and *CD44* expression in (G) MPE, (H) peripheral blood, and (I) surgically resected *EGFR*-mutant lung adenocarcinoma. The correlation analysis was performed according to Pearson's correlation method.
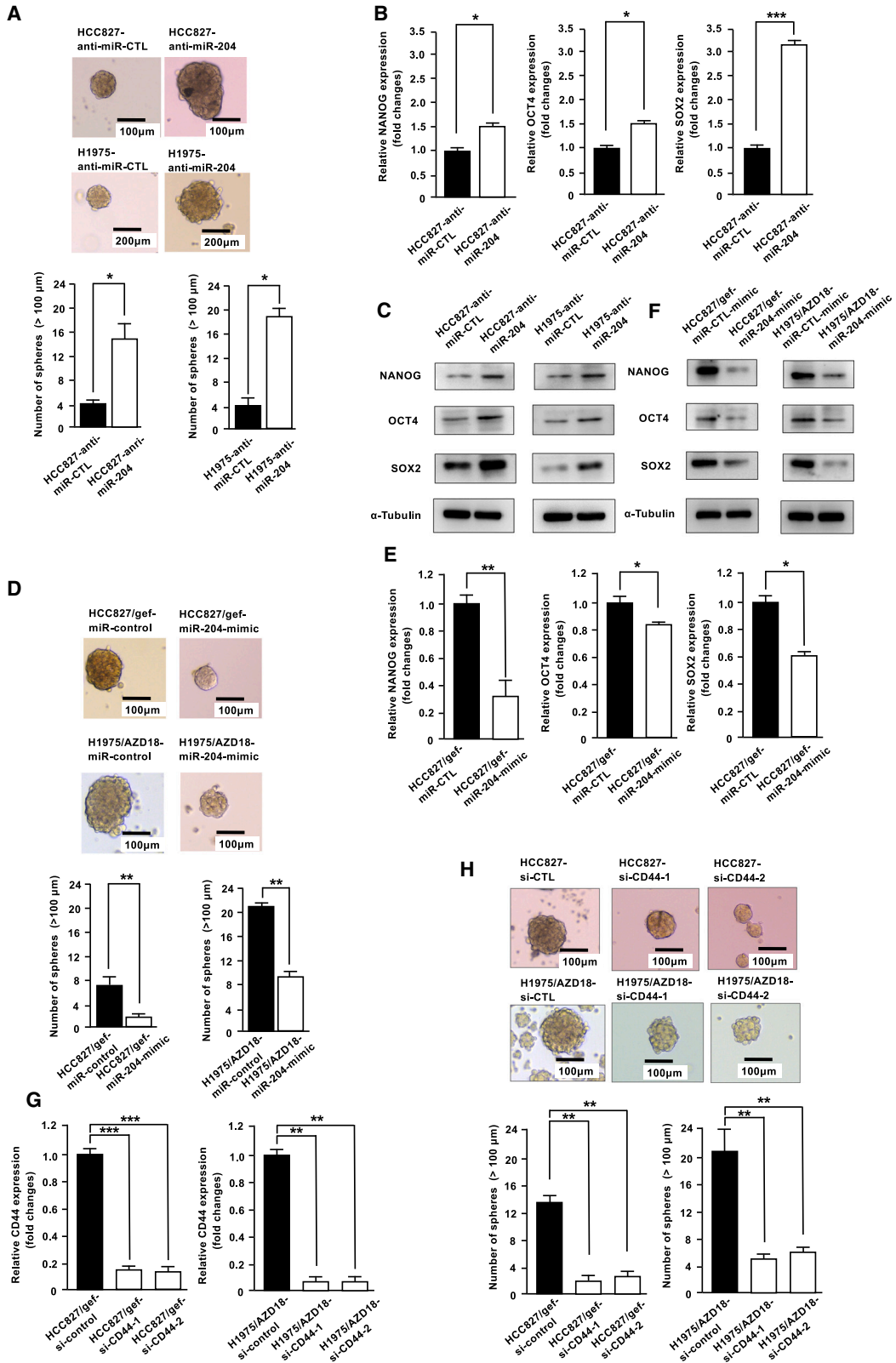
(legend on next page)

cell migration and invasion compared to control cells (Figures 5C and 5D). Suppression of miR-204 in osimertinib-sensitive cells enhanced the mRNA levels of EMT regulators (Snail, Slug, and Zeb1) (Figure S6), and increased the protein expression of vimentin, N-cadherin, and Snail (mesenchymal cell marker) but attenuated E-cadherin (epithelial cell marker) protein expression (Figure 5E).

Furthermore, suppression of *CD44* expression in HCC827/gef and H1975/AZD-18 (HCC827/gef-siCD44-1, HCC827/gef-siCD44–2, H1975/AZD-18-siCD44-1, and H1975/AZD-18-siCD44-2) reduced lung cancer cell migration and invasion and is indicated in Figures 5F and 5G. miR-204-attenuated lung cancer cell migration and invasion may act through the suppression of *CD44*.

After knocking down *CD44* in osimertinib-resistant cells (H1975/AZD-18-siCD44–1, H1975/AZD-18-siCD44-2, HCC827/gef-siCD44-1, and HCC827/gef-siCD44-2) using siRNA, CD44 protein expression was attenuated. Western blot analysis showed that E-cadherin expression was significantly increased, whereas N-cadherin, vimentin, and Snail (mesenchymal markers) were significantly attenuated (Figure 5H). However, upregulating CD44 expression in osimertinib-sensitive cells (H1975-CD44) suppressed E-cadherin expression but enhanced N-cadherin, vimentin, and Snail expression (Figure 5I). These results suggest that miR-204/CD44 plays an important role in regulating EMT in lung cancer cells.

Inhibition of *CD44* restored osimertinib sensitivity in osimertinib-resistant lung cancer cells
The two *CD44*-specific-siRNAs (si-CD44-1 and si-CD44-2) were used to knock down *CD44* expression in osimertinib-resistant cells (HCC827/gef and H1975/AZD18) (Figure 6A). After transfection, the *CD44*-knockdown transfectants (HCC827/gef-si-CD44-1 and -2 and H1975/gef-siCD44-1 and -2) or control transfectants (HCC827/gef-si-control and H1975/gef-si-control) were exposed to osimertinib, and cell viability was analyzed by MTT assay. The results indicated that inhibition of *CD44* expression remarkably restored osimertinib sensitivity in osimertinib-resistant lung cancer cells (Figure 6B).

Restoration of *CD44* reversed the effects of miR-204 on osimertinib sensitivity
The upregulation of miR-204 in osimertinib-resistant cells promoted osimertinib-induced cell death and enhanced osimertinib sensitivity (Figure 2), whereas elevated *CD44* attenuated osimertinib sensitivity in miR-204-expression transfectants (H1975/AZD18-Lentic-miR204-CD44) (Figure 6C). Western blotting showed that upregulating miR-204 expression in osimertinib-resistant cells (H1975/AZD18) attenuated the protein expression of CD44, SOX2,

N-cadherin, vimentin, and Snail but enhanced E-cadherin expression. Furthermore, CD44 expression in miR-204-overexpression transfectants (H1975/AZD18-Lenti-miR-204) subsequently increased the expression of SOX2, vimentin, N-cadherin, and Snail but attenuated E-cadherin expression (Figure 6D). After statistically analyzing the protein band signals from triplicate western blots using ImageJ, we found that miR-204-expression transfectants had significantly lower vimentin expression than did control transfectants. However, miR-204-CD44-expression transfectants had significantly higher vimentin expression than did miR-204-expression transfectants (Figure S7). These results suggest that the restoration of *CD44* reverses the effects of miR-204 on osimertinib sensitivity. miR-204 represses cancer stemness and increases osimertinib sensitivity in lung cancer cells by targeting *CD44*.

High miR-204/low CD44 was associated with longer overall survival in lung cancer patients
To explore the impact of miR-204 on overall survival (OS) in lung adenocarcinoma, we collected surgical specimens from 40 patients with early-stage lung adenocarcinoma and analyzed the relationship between miR-204 expression level and OS. Patients who received adjuvant chemotherapy were excluded. Table S5 shows the clinical characteristics of the patients.

Patients with lung adenocarcinoma with high miR-204 expression (n = 20) had a longer time-to-tumor recurrence (TTP) than those with low miR-204 expression (n = 20) (median TTP not yet reached versus 22.3 months; p = 0.046) (Figure 6E). In addition, the high miR-204 patient group had a significantly longer OS (median OS not yet reached) than the low miR-204 group (73.1 months; p = 0.020) (Figure 6F).

We also analyzed the survival data of lung adenocarcinoma patients from The Cancer Genome Atlas (TCGA) database. Of the 351 early lung adenocarcinoma patients, there were no differences in clinical characteristics between the high and low miR-204 groups (Table S6). The high miR-204 patient group had a significantly longer OS (59.1 months) than the low miR-204 group (42.4 months; p = 0.034) (Figure 6G).

Furthermore, we explored the OS of lung adenocarcinoma patients from the Kaplan-Meier plotter for lung cancer database (http://kmplot.com/analysis/index.php?p=service&cancer=pancancer_mirna). Patients with higher miR-204 expression had a longer median OS than those with lower miR-204 expression (HR = 0.71, 95% CI 0.53–0.95; p = 0.021) (Figure 6H). In contrast, patients with higher *CD44* expression had a shorter median disease-free survival (54.0 months versus 104.9 months; p = 1.9e−5) (Figure 6I) and median

Figure 4. MiR-204 reduced lung cancer stemness
(A, D, and H) Tumor spheroid formation assays were used to evaluate cancer stemness phenotype (*p < 0.05; **p < 0.01). (B and E) The expressions of cancer stem stemness markers (NANOG, OCT4, and SOX2) were detected by qRT-PCR (*p < 0.05; **p < 0.01; ***p < 0.001). (C and F) The expression levels of NANOG, OCT4, and SOX2 were determined by western blots. (G) qRT-PCR was performed to measure the expression levels of CD44 after transient silencing of CD44 in HCC827/gef or H1975/AZD 18 cells (**p < 0.01; ***p < 0.001). p values were determined by Student's t test.
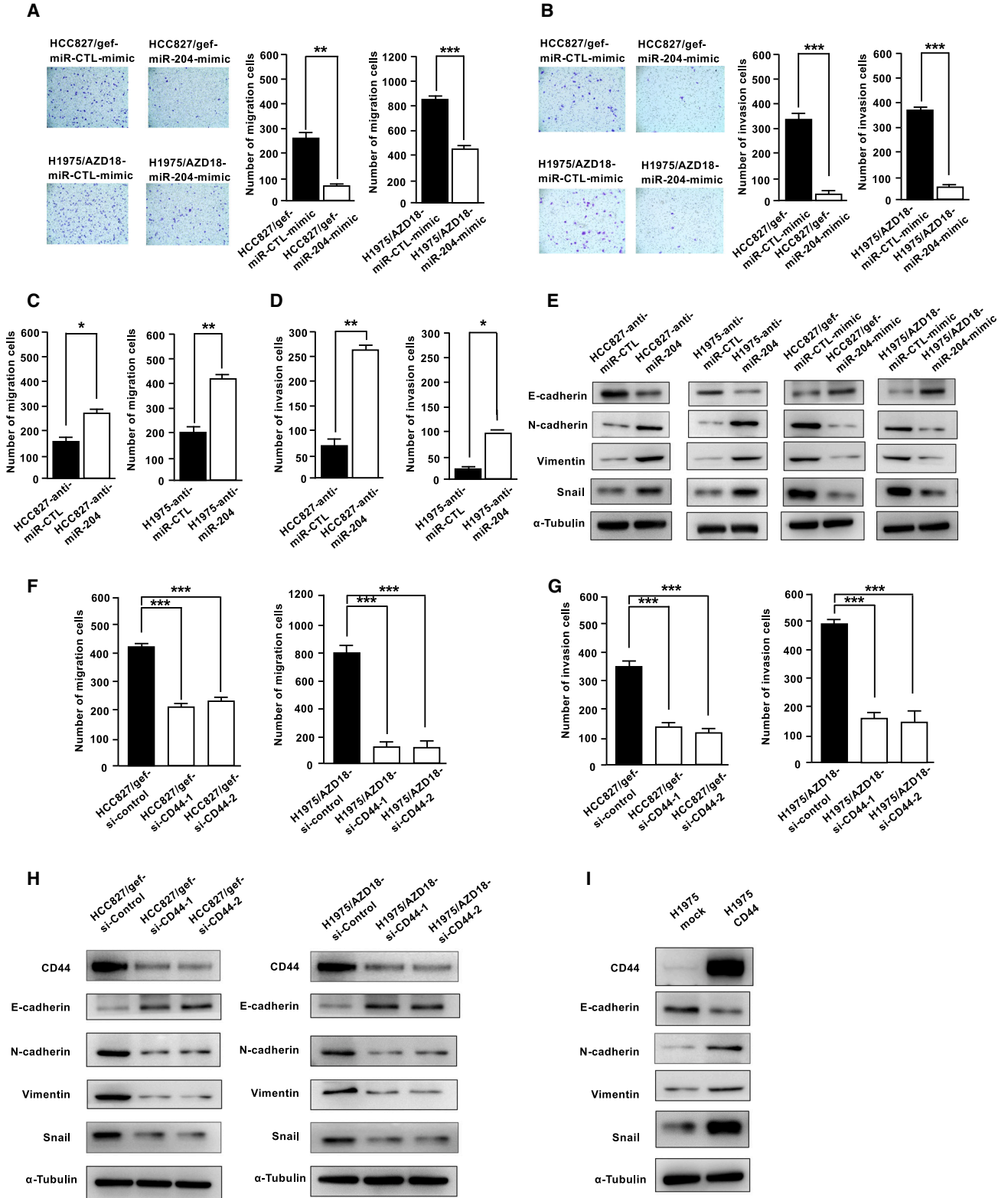
(legend on next page)

OS (87.7 months versus 117.3 months; p = 0.0043) than patients with lower *CD44* expression (Figure 6J).

DISCUSSION

In this study, we demonstrated for the first time that miR-204 contributes to osimertinib sensitivity in lung cancer. miR-204 expression was remarkably decreased in osimertinib-resistant lung cancer cell lines and in MPEs of lung adenocarcinoma after resistance to osimertinib (Figure 1). We also revealed that lung cancer patients with tumors with higher miR-204 levels or higher serum miR-204 levels had longer median PFS with EGFR-TKIs than those with lower miR-204 levels (Figure 1). *In vitro* and *in vivo*, the overexpression of miR-204 in osimertinib-resistant lung cancer cells restored osimertinib sensitivity and enhanced osimertinib-induced cell death (Figure 2) In contrast, the suppression of miR-204 confers resistance of osimertinib in osimertinib-sensitive cells.

miR-204 was identified as a tumor suppressor in various cancers. miR-204 acts as a tumor suppressor in breast cancer by targeting FOXA1,[40] and lower miR-204 expression was associated with shorter PFS and OS.[32] In hepatocellular carcinoma, miR-204 expression is remarkably repressed compared to that in adjacent liver tissues. miR-204 inhibits human hepatocellular carcinoma progression by directly targeting Zeb2.[33] *IGF2BP2*, a miR-204 direct target gene, was verified in thyroid cancer, and the miR-204/*IGF2BP2* signaling axis has been demonstrated to play a critical role in thyroid cancer progression.[34] Moreover, miR-204 expression was detected in plasma samples from patients with NSCLC and healthy controls. The results showed that miR-204 levels in NSCLC plasma remarkably correlated with tumor stage and distant metastasis, and lower plasma levels of miR-204 were associated with poor overall and disease-free survival.[31] These data were compatible with our study showing that the miR-204 in surgical lung cancer specimens correlated with relapse-free survival and OS. However, the molecular mechanisms through which miR-204 is involved in lung cancer development and progression are not fully understood. Our results revealed that miR-204 attenuated lung cancer cell stemness, migration, and invasion through the CD44 signaling pathway (Figures 4 and 5). The expression of miR-204 in osimertinib-resistant cells promoted osimertinib-induced cell death and enhanced osimertinib sensitivity (Figure 2), whereas elevated CD44 attenuated osimertinib sensitivity in miR-204-overexpressing transfectants (H1975/AZD18-Lentic-miR204-CD44; Figure 6). The miR-204/CD44 axis contributes to cancer stemness, EMT phenotypic changes, and EGFR-TKI resistance. Therefore, miR204 and CD44 are potential molecular targets in lung cancer cells.

CD44, a nonkinase transmembrane receptor for the binding of hyaluronan and other extracellular matrix molecules, has been implicated in a variety of physiological events, including cytoskeletal architecture reorganization, cell homing, and lymphocyte activation. CD44 expression has been strongly linked to tumorigenesis, EMT, and cancer stemness.[41] Activated CD44 is coupled with cytoskeletal elements or specific signaling adaptor proteins that activate various cellular signaling pathways, including transforming growth factor-β, Hippo, β-catenin, EGFR, and signal transducer and activator of transcription 3 signaling pathways.[42,43] Studies have reported that CD44 promotes the EMT phenotype in breast cancer, colon cancer, pancreatic cancer, and lung cancer.[42–44] The overexpression of CD44 promotes tumorigenesis, EMT phenotypic changes, metastatic potential, and upregulation of EGFR signaling pathways in breast cancer.[45] Previous studies have demonstrated that silencing *CD44* in lung cancer inhibits cell growth and induces apoptosis by deactivating EGFR signaling.[46] These studies also indicated that knockdown of *CD44* increased the sensitivity of *EGFR* WT NSCLC cells to cisplatin.[46] Furthermore, other studies revealed that CD44 expression was substantially higher in EGFR-TKI-resistant lung cancer cells (HCC827EPR and HCC827CNXR-S4 cells) than in parental controls (HCC827 cells). This report also indicated that some *EGFR*-mutant lung cancer cells (H1975 and HCC4006) with high CD44 expression tend to acquire resistance to EGFR-TKIs by facilitating EMT.[43] The authors suggested that CD44 expression is necessary for EMT phenotype acquisition, but high CD44 expression alone is not sufficient to convert epithelial cells to mesenchymal cells.[43] Understanding the molecular mechanisms that regulate CD44 expression can provide new insights into the development of novel strategies for lung cancer therapy. In the present study, we demonstrated that CD44 was a direct downstream target of miR-204 in lung cancer cells (Figure 3). Higher CD44 expression was detected in osimertinib-resistant lung cancer cells (HCC827/gef and H1975/AZD18) than in the parental controls (HCC827 and H1975; Figure 3). Depletion of CD44 expression in miR-204-low expressed-osimertinib-resistant cells restored osimertinib sensitivity, as well as inhibited sphere formation and cell migration/invasion (Figures 4, 5, and 6). Our results also suggested that miR-204/CD44 is essential for conferring osimertinib resistance and enhancing cancer stemness and EMT in lung cancer cells.

In conclusion, miR-204 reversed osimertinib resistance by targeting CD44 signaling and suppressing cancer stemness and the EMT phenotype. The miR-204/CD44 axis plays an important role in overcoming osimertinib resistance in lung cancer; these results provide the groundwork for the development of osimertinib resistance–reversing therapeutic methods.

Figure 5. miR-204 inhibited lung cancer cell migration and invasion abilities through targeting CD44

(A, C, and F) *In vitro* cell migration ability was evaluated using transwell assays without Matrigel (*p < 0.05; **p < 0.01; ***p < 0.001). (B, D, and G) *In vitro* cell invasion ability was determined using transwell assays with Matrigel (*p < 0.05; **p < 0.01; ***p < 0.001) The detailed procedures of *in vitro* cell migration and invasion abilities have been described previously.[20] (E) The protein expression of EMT markers E-cadherin and vimentin was determined by western blotting. (H and I) Knockdown (H) and (I) upregulated CD44 expression changed EMT markers. The protein expression of EMT markers E-cadherin, N-cadherin, vimentin, and Snail were determined by western blotting. p values were determined by Student's t test.
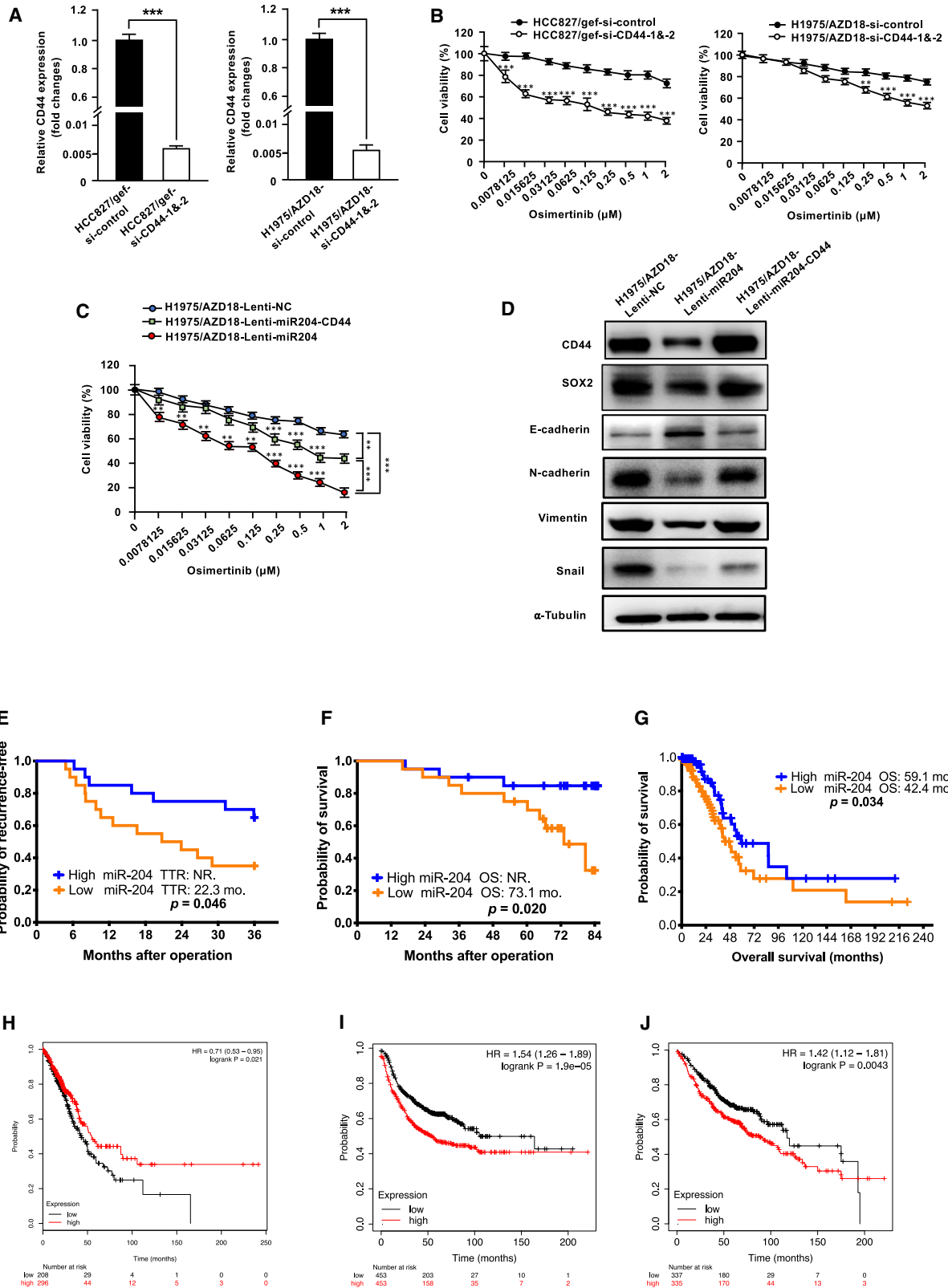
(legend on next page)

MATERIALS AND METHODS

Cell lines

The human lung cancer cell lines HCC827 and H1975 were acquired from the American Type Culture Collection (ATCC, Manassas, VA). The PC9 human lung cancer cell line and its derivative gefitinib-resistant subline (PC9/gef) were provided by Prof. James Chih-Hsin Yang, as described previously.[47] The osimertinib-resistant cells (HCC827/gef, PC9/gef, and H1975/AZD) were selected from the parental cells (HCC827, PC9, and H1975) after continuous exposure to the EGFR-TKIs according to a dose-escalation procedure. Briefly, PC9/gef (pooled clones) with gefitinib resistance ($IC_{50} > 1$ μM) was isolated after being grown in culture media containing escalating concentrations of gefitinib for 6 months.[47,48] HCC827/gef was selected after exposure to stepwise escalating concentrations of gefitinib up to 10 μM.[19] PC9/gef and HCC827/gef cells were cross-resistant to osimertinib. No acquired T790M mutation or c-Met amplification was detected in both PC9/gef and HCC827/gef. H1975 cells harboring EGFR L858R and T790M mutations are resistant to first-generation EGFR-TKI treatment (gefitinib and erlotinib) but sensitive to osimertinib treatment ($IC_{50} < 0.02$ μM). The osimertinib-resistant subline H1975/AZD was derived from the H1975 cell line treated with osimertinib (AZD9291) for ~6 months by increasing osimertinib concentration up to 3 μM.[49] Osimertinib-resistant H1975/AZD15 and H1975/AZD18 were single clones isolated from H1975/AZD mixed clones using a serial dilution method.

A lentivirus system was used to construct stable miR-204 expression clones. Lentivector-based miR-204 precursor constructs (catalog no. PMIRH204-AA-1) and control vector were purchased from System Biosciences. The constitutive expression of miR-204 in osimertinib-resistant cells (H1975/AZD18-Lenti-miR-204; H1975/AZD18 cells transfected with Lenti-miR-204 expression construct) and negative control cells (H1975/AZD18-Lenti-NC) was established. All of the human cell lines were free of mycoplasma contamination and authenticated using short tandem repeat profiling. RPMI-1640 medium supplemented with 10% fetal bovine serum (FBS) was used for cell lines culture at 37°C in a humidified 5% CO_2 incubator.

Quantitative real-time reverse transcription PCR

TRIzol reagent was used to extract RNA from the cell lines. Then, the RNA reverse transcribed to cDNA using random primers and MultiScribe reverse transcriptase, according to the manufacturer's protocol (Invitrogen/Thermo Fisher Scientific, Waltham, MA). qRT-PCR was performed on a QuantStudio 7 flex real-time PCR system (Thermo Fisher Scientific) using a standard protocol with TATA box-binding protein (TBP) or RNU6B (Thermo Fisher Scientific, catalog no. 4427975; assay ID 001093) as an internal control for mRNA and miRNA, respectively. The primers used for the different genes in the present study are listed in Table S7.

Western blotting

Protein samples of the cells were extracted using radioimmunoprecipitation assay buffer (Cell Signaling Technology, Danvers, MA). Cell lysates were prepared and quantified using the Pierce BCA protein assay kit (Thermo Fisher Scientific). The obtained proteins (30–100 μg) were subjected to SDS-PAGE, transferred to a polyvinylidene fluoride membrane, and incubated with the indicated primary antibodies. Then, we incubated the blot with horseradish peroxidase–linked secondary antibodies, and immunoreactive signals were visualized using SuperSignal West Pico PLUS Chemiluminescent Substrate (Thermo Fisher Scientific). The different antibodies and their concentrations for the various genes used for western blot analysis are listed in Table S8.

Cytotoxicity tests

To evaluate the cytotoxic effects of the EGFR-TKIs (gefitinib and osimertinib), the colorimetric MTT assay was used. Briefly, we plated 3,000 cells per well in 96-well plates and treated with the indicated drugs. After 72 h, 10 μL MTT reagent (0.5 mg/mL) was added to each well containing the samples in 100 μL of culture medium and then was incubated for another 3 h at 37°C. Finally, 100 μL of DMSO was added to each well to stop the reaction, and the absorbance was measured at 570 nm using a SpectraMax i3x Multi-Mode Microplate Reader (Molecular Devices, San Jose, CA).

Caspase activity assay

Apoptosis protein markers, such as BIM, cleaved caspase-3, and PARPs, were detected by western blotting. Activity of caspase-9 was measured using a luminescent Caspase-Glo 9 assay kit according to the manufacturer's instructions (Promega, Madison, WI). Cells were seeded in 96-well plates, allowed to grow for 24 h at 37°C, and subsequently treated with EGFR-TKIs for 24 h. After incubation, the cells were lysed. In this assay, caspase was released and the luminogenic substrate containing the L-Leucyl-L-Glutamyl-L-Histidyl-L-Aspartate (LEHD) sequence was recognized. The substrate was

Figure 6. Restoration of CD44 expression reversed the effects of miR-204 on osimertinib sensitivity and cancer stemness
(A) The CD44 expression was detected by qRT-PCR (*p < 0.05). (B and C) The cellular viability in CD44-knockdown and CD44-restoration transfectants was determined following treatment with various doses of osimertinib for 96 h in MTT assays (**p < 0.01; ***p < 0.001). (D) The expression of CD44, Sox2, E-cadherin, and vimentin was determined by western blotting. Here, HCC827/gef-si-CD44-1 and -2 and H1975/gef-siCD44-1 and -2 were CD44-knockdown transfectants, whereas H1975/AZD18-Lentic-miR204-CD44 were represented as CD44-restored transfectants. p values were determined by Student's t test. (E and F) Patients of lung adenocarcinoma with high miR-204 expression (n = 20) had (E) a longer TTP (not yet reached versus 22.3 months; p = 0.046) and (F) a longer OS (not yet reached versus 73.1 months; p = 0.020) than those with low miR-204 expression (n = 20). (G) Of the 351 early-stage lung adenocarcinoma patients from TCGA database, the high miR-204 patient group had a significantly longer OS (59.1 months) than the low miR-204 group (42.4 months; p = 0.034). (H) From the Kaplan-Meier plotter for lung cancer database, patients with higher miR-204 expression had a longer median OS than those with lower miR-204 expression (p = 0.021). (I and J) Patients with higher CD44 expression had a (I) shorter median disease-free survival (54.0 months versus 104.9 months; p = 1.9e−5), and (J) OS (87.7 months versus 117.3 months; p = 0.0043) than patients with lower CD44 expression. NR, not reached.

cleaved by activated caspase, and then the substrate for luciferase was released. Finally, a SpectraMax i3x Multi-Mode Microplate Reader (Molecular Devices) was used to measure luminescence.

Gene knockdown

Gene knockdown was achieved by adding miR-204 inhibitors (MH11116, Thermo Fisher Scientific) or by transfecting cells with gene-specific siRNA (si-CD44) (Thermo Fisher Scientific). Approximately 2×10^5 cells were seeded in 2 mL RPMI medium with 10% FBS in 6-well plates 24 h before transfection. Cells were transfected with siRNAs at a concentration of 65 nM using Lipofectamine RNAiMAX Transfection Reagent (Thermo Fisher Scientific), according to the manufacturer's instructions. After 48 h, gene expression levels were evaluated by qRT-PCR and western blotting.

Luciferase reporter assays

To clone fragments of the potential downstream target genes of miR-204, a PCR-based method was used. Specific primers were designed using a bioinformatics search in GenBank. Total RNA was extracted from the H1975 cell line, and the cDNA library was obtained. We amplified the 3′ UTR of the *CD44* gene sequence from the cDNA library and cloned it into the pMIR-REPORT miRNA expression reporter vector (Applied Biosystems, Foster City, CA). A mutant 3′ UTR of *CD44* harboring a mutant sequence of the miR-204 binding site was constructed by the QuikChange Site-Directed Mutagenesis Kit (Stratagene, La Jolla, CA). The cells were cultured in 24-well plates at a density of 3×10^4 cells per well for 24 h before transfection. Subsequently, cells were transfected with a Luc-putative gene vector or Luc-putative gene mutation vector. Luciferase activity was measured using a dual-luciferase reporter assay system (Promega) after 24 h of incubation.

Sphere formation or self-renewal assays

After manipulation of miR-204 expression levels in osimertinib-sensitive or osimertinib-resistant cells, the cells were cultured at a density of 5,000 cells/well in 24-well ultralow attachment plates (Corning, Corning, NY) at 37°C in serum-free DMEM/Nutrient Mixture F-12 (DMEM/F12) (1:1) (Gibco Life Science, Great Island, NY), supplemented with 1% penicillin/streptomycin, $1 \times$ B27 (Gibco Life Science), 4 mM HEPES (Sigma-Aldrich, St. Louis, MO), 20 ng/mL basic fibroblast growth factor (PeproTec, Rocky Hill, NJ), 20 ng/mL EGF (PeproTec), and $1 \times$ insulin-transferrin-sodium selenite (Sigma-Aldrich). Growth factor–enriched conditions were maintained by adding supplements every 2 days. The total number and size of spheres were analyzed on day 7. Images of the spheres were obtained using an EVOS imaging system (Thermo Fisher Scientific).

Animal models

The animal study procedures were also approved by the Institutional Animal Care and Use Committee of the National Taiwan University College of Medicine. Cancer cells, including H1975/AZD18-Lenti-miR-204 and H1975/AZD18-Lenti-NC, were injected subcutaneously into the lower rear flank of 4- to 6-week-old severe combined immunodeficient athymic male mice. Tumor volumes were evaluated after treatment with osimertinib (0 or 4 mg/kg). Tumor volume and mouse weight were recorded every 2 days. The excision tumor samples were evaluated for Ki-67 (1:1,000, polyclonal antibody, ProteinTech, Wuhan, China) by immunohistochemical stain. In addition, the ApopTag Peroxidase In Situ Apoptosis Detection Kit (no. S7100, Merck Millipore, Darmstadt, Germany) was used to detect the apoptotic cells of the animal tumor specimens by a terminal deoxynucleotidyl transferase–mediated deoxyuridine TUNEL procedure according to the manufacturer's instructions.

MPE isolation

In the chest ultrasonography examination room at the National Taiwan University Hospital (NTUH), pleural effusions were consecutively collected from patients who underwent thoracentesis. An informed consent form for future molecular analyses was signed by all of the patients before thoracentesis. This study was approved by the institutional review board (IRB) of NTUH. MPE related to lung adenocarcinoma was used in this study. The pleural fluids of the patients were aseptically acquired in vacuum bottles by thoracentesis. Red blood cell (RBC) lysis buffer was used to homolyze RBCs in the pleural effusions. PBS were used to wash the remaining cells twice, and the cells were cultured in complete RPMI-1640 media.[50] The medium was replaced every 2–3 days. After 10 days, the cells were harvested. TRIzol reagent (Invitrogen) was used to extract total RNA from cultured cells. The expression of miR-204 was determined using qRT-PCR. qRT-PCR was performed using TaqMan miR-204 probes (Thermo Fisher Scientific, catalog no. 4427975; assay ID 000508) on an Applied Biosystems 7500 Sequence Detection System.

Plasma and tissue procurement

Peripheral blood samples were taken from patients with advanced *EGFR*-mutant lung adenocarcinoma who received EGFR-TKIs as a first-line single-agent treatment. Plasma was collected, aliquoted, and frozen at −80°C until use.

Surgical excision tumor specimens from patients with early lung cancer were collected at the NTUH. The IRB of NTUH approved the study protocols, and informed consent was obtained from all of the surgically treated patients before the procedure.

We evaluated the expression of miR-204 by qRT-PCR in resected lung cancer tissue and correlated its expression with clinical characteristics (stage, lymph node metastasis, and cancer recurrence) and OS of lung cancer patients.

Plasma RNA isolation and miRNA qRT-PCR assay

Fluid RNA isolation and miRNA Q-PCR were conducted to analyze the miR-204 content in blood. Briefly, blood samples were collected from each donor and processed within 1 h. Plasma was isolated by centrifugation at 3,000 rpm ($1,800 \times g$) for 10 min at 4°C. The supernatant plasma was collected and stored at −30°C until analysis. Total RNA was extracted from 600 μL of plasma using the miRNeasy Serum/Plasma Kit (Qiagen, Venlo, the Netherlands) according to the manufacturer's instructions. qRT-PCR was performed using a

TaqMan miRNA PCR kit (Applied Biosystems) following the manufacturer's instructions. Briefly, 60 ng of total RNA was reverse transcribed into cDNA using the High-Capacity cDNA Reverse Transcription Kit (Applied Biosystems) and stem-loop RT primers (Applied Biosystems). RT-PCR was performed using TaqMan miRNA probes (Applied Biosystems) on an Applied Biosystems 7500 Sequence Detection System. After the reactions, cycle threshold (CT) values were determined using fixed threshold settings (0.1). To calculate the absolute expression levels of the target miRNAs, a series of synthetic miRNA oligonucleotides of known concentrations (0.02–300 fmol) were also reverse transcribed and amplified. The absolute amount of each miRNA was calculated using a standard curve. Because there is no current consensus on housekeeping miRNAs for qRT-PCR analysis of plasma miRNAs, the expression levels of miRNAs were directly normalized to plasma volume in our study.

Statistical analysis

SPSS (version 22.0; IBM SPSS Statistics, Armonk, NY) was adopted for statistical analysis. Pearson's χ^2 test was used to analyze categorical variables, and Fisher's exact test was used when the sample variables were ≤ 5. The PFS was compared using the log rank test and plotted using the Kaplan-Meier method. The correlation analysis was performed according to Pearson's correlation method. Two-sided $p < 0.05$ was considered significant.

DATA AND CODE AVAILABILITY

Please contact the corresponding author for data requests.

SUPPLEMENTAL INFORMATION

Supplemental information can be found online at https://doi.org/10.1016/j.omtn.2023.102091.

AUTHOR CONTRIBUTIONS

S.-G.W., T.-H.C., and J.-Y.S. designed this study. T.-H.C. and Y.-N.L. performed the genetic mutation analysis. S.-G.W., M.-F.T., and J.-Y.S. analyzed the data and wrote the paper. Y.-L.H. performed the pathological diagnosis. C.-L.H. performed the bioinformatics analysis. All of the authors read and approved the final manuscript.

DECLARATION OF INTERESTS

S.-G.W. received speaking honoraria from Eli Lilly, Boehringer Ingelheim, Merck Sharp & Dohme, Novartis, Bristol-Myers Squibb, AstraZeneca, Pfizer, and Roche. J.-Y.S. has received honoraria from Bristol-Myers Squibb, AstraZeneca, Boehringer Ingelheim, Roche, Eli Lilly, Merck Sharp & Dohme, Pfizer, Chugai Pharmaceutical, Novartis, and Ono Pharmaceutical; personal fees for advisory boards from Boehringer Ingelheim, Roche, Merck Sharp & Dohme, Eli Lilly, Ono Pharmaceutical, Bristol-Myers Squibb, AstraZeneca, and Chugai Pharmaceutical; and travel expenses from Bristol-Myers Squibb, Pfizer, Roche, Chugai Pharmaceutical, and Merck Sharp & Dohme. The remaining authors declare no competing interests.

REFERENCES

1. Siegel, R.L., Miller, K.D., Wagle, N.S., and Jemal, A. (2023). Cancer statistics, 2023. CA A Cancer J. Clin. 73, 17–48.

2. Thai, A.A., Solomon, B.J., Sequist, L.V., Gainor, J.F., and Heist, R.S. (2021). Lung cancer. Lancet 398, 535–554.

3. Rossi, A., and Di Maio, M. (2016). Platinum-based chemotherapy in advanced non-small-cell lung cancer: optimal number of treatment cycles. Expert Rev. Anticancer Ther. 16, 653–660.

4. Cheng, W.L., Feng, P.H., Lee, K.Y., Chen, K.Y., Sun, W.L., Van Hiep, N., Luo, C.S., and Wu, S.M. (2021). The Role of EREG/EGFR Pathway in Tumor Progression. Int. J. Mol. Sci. 22, 12828.

5. Rosell, R., Moran, T., Queralt, C., Porta, R., Cardenal, F., Camps, C., Majem, M., Lopez-Vivanco, G., Isla, D., Provencio, M., et al. (2009). Screening for epidermal growth factor receptor mutations in lung cancer. N. Engl. J. Med. 361, 958–967.

6. Shi, Y., Au, J.S.K., Thongprasert, S., Srinivasan, S., Tsai, C.M., Khoa, M.T., Heeroma, K., Itoh, Y., Cornelio, G., and Yang, P.C. (2014). A prospective, molecular epidemiology study of EGFR mutations in Asian patients with advanced non-small-cell lung cancer of adenocarcinoma histology (PIONEER). J. Thorac. Oncol. 9, 154–162.

7. Mok, T.S., Wu, Y.L., Thongprasert, S., Yang, C.H., Chu, D.T., Saijo, N., Sunpaweravong, P., Han, B., Margono, B., Ichinose, Y., et al. (2009). Gefitinib or carboplatin-paclitaxel in pulmonary adenocarcinoma. N. Engl. J. Med. 361, 947–957.

8. Wu, S.G., Liu, Y.N., Tsai, M.F., Chang, Y.L., Yu, C.J., Yang, P.C., Yang, J.C.H., Wen, Y.F., and Shih, J.Y. (2016). The mechanism of acquired resistance to irreversible EGFR tyrosine kinase inhibitor-afatinib in lung adenocarcinoma patients. Oncotarget 7, 12404–12413.

9. Yu, H.A., Arcila, M.E., Rekhtman, N., Sima, C.S., Zakowski, M.F., Pao, W., Kris, M.G., Miller, V.A., Ladanyi, M., and Riely, G.J. (2013). Analysis of tumor specimens at the time of acquired resistance to EGFR-TKI therapy in 155 patients with EGFR-mutant lung cancers. Clin. Cancer Res. 19, 2240–2247.

10. Mok, T.S., Wu, Y.L., Ahn, M.J., Garassino, M.C., Kim, H.R., Ramalingam, S.S., Shepherd, F.A., He, Y., Akamatsu, H., Theelen, W.S.M.E., et al. (2017). Osimertinib or Platinum-Pemetrexed in EGFR T790M-Positive Lung Cancer. N. Engl. J. Med. 376, 629–640.

11. Soria, J.C., Ohe, Y., Vansteenkiste, J., Reungwetwattana, T., Chewaskulyong, B., Lee, K.H., Dechaphunkul, A., Imamura, F., Nogami, N., Kurata, T., et al. (2018). Osimertinib in Untreated EGFR-Mutated Advanced Non-Small-Cell Lung Cancer. N. Engl. J. Med. 378, 113–125.

12. Leonetti, A., Sharma, S., Minari, R., Perego, P., Giovannetti, E., and Tiseo, M. (2019). Resistance mechanisms to osimertinib in EGFR-mutated non-small cell lung cancer. Br. J. Cancer 121, 725–737.

13. Thress, K.S., Paweletz, C.P., Felip, E., Cho, B.C., Stetson, D., Dougherty, B., Lai, Z., Markovets, A., Vivancos, A., Kuang, Y., et al. (2015). Acquired EGFR C797S mutation mediates resistance to AZD9291 in non-small cell lung cancer harboring EGFR T790M. Nat. Med. 21, 560–562.

14. Schmid, S., Li, J.J.N., and Leighl, N.B. (2020). Mechanisms of osimertinib resistance and emerging treatment options. Lung Cancer 147, 123–129.

15. Rupaimoole, R., and Slack, F.J. (2017). MicroRNA therapeutics: towards a new era for the management of cancer and other diseases. Nat. Rev. Drug Discov. 16, 203–222.

16. Saliminejad, K., Khorram Khorshid, H.R., Soleymani Fard, S., and Ghaffari, S.H. (2019). An overview of microRNAs: Biology, functions, therapeutics, and analysis methods. J. Cell. Physiol. 234, 5451–5465.

17. Wu, S.G., Chang, T.H., Liu, Y.N., and Shih, J.Y. (2019). MicroRNA in Lung Cancer Metastasis. Cancers 11, 265.

18. Naidu, S., and Garofalo, M. (2015). microRNAs: An Emerging Paradigm in Lung Cancer Chemoresistance. Front. Med. *2*, 77.

19. Liu, Y.N., Tsai, M.F., Wu, S.G., Chang, T.H., Tsai, T.H., Gow, C.H., Wang, H.Y., and Shih, J.Y. (2020). miR-146b-5p Enhances the Sensitivity of NSCLC to EGFR Tyrosine Kinase Inhibitors by Regulating the IRAK1/NF-kappaB Pathway. Mol. Ther. Nucleic Acids *22*, 471–483.

20. Wang, H.Y., Liu, Y.N., Wu, S.G., Hsu, C.L., Chang, T.H., Tsai, M.F., Lin, Y.T., and Shih, J.Y. (2020). MiR-200c-3p suppression is associated with development of acquired resistance to epidermal growth factor receptor (EGFR) tyrosine kinase inhibitors in EGFR mutant non-small cell lung cancer via a mediating epithelial-to-mesenchymal transition (EMT) process. Cancer Biomarkers *28*, 351–363.

21. Li, X., Chen, C., Wang, Z., Liu, J., Sun, W., Shen, K., Lv, Y., Zhu, S., Zhan, P., Lv, T., and Song, Y. (2021). Elevated exosome-derived miRNAs predict osimertinib resistance in non-small cell lung cancer. Cancer Cell Int. *21*, 428.

22. Hisakane, K., Seike, M., Sugano, T., Yoshikawa, A., Matsuda, K., Takano, N., Takahashi, S., Noro, R., and Gemma, A. (2021). Exosome-derived miR-210 involved in resistance to osimertinib and epithelial-mesenchymal transition in EGFR mutant non-small cell lung cancer cells. Thorac. Cancer *12*, 1690–1698.

23. Li, T., Pan, H., and Li, R. (2016). The dual regulatory role of miR-204 in cancer. Tumour Biol. *37*, 11667–11677.

24. Conte, I., Hadfield, K.D., Barbato, S., Carrella, S., Pizzo, M., Bhat, R.S., Carissimo, A., Karali, M., Porter, L.F., Urquhart, J., et al. (2015). MiR-204 is responsible for inherited retinal dystrophy associated with ocular coloboma. Proc. Natl. Acad. Sci. USA *112*, E3236–E3245.

25. Bereimipour, A., Najafi, H., Mirsane, E.S., Moradi, S., and Satarian, L. (2021). Roles of miR-204 in retinal development and maintenance. Exp. Cell Res. *406*, 112737.

26. Sun, Y., Koo, S., White, N., Peralta, E., Esau, C., Dean, N.M., and Perera, R.J. (2004). Development of a micro-array to detect human and mouse microRNAs and characterization of expression in human organs. Nucleic Acids Res. *32*, e188.

27. Rudnicki, M., Perco, P., D Haene, B., Leierer, J., Heinzel, A., Mühlberger, I., Schweibert, N., Sunzenauer, J., Regele, H., Kronbichler, A., et al. (2016). Renal microRNA- and RNA-profiles in progressive chronic kidney disease. Eur. J. Clin. Invest. *46*, 213–226.

28. Liu, Y., Usa, K., Wang, F., Liu, P., Geurts, A.M., Li, J., Williams, A.M., Regner, K.R., Kong, Y., Liu, H., et al. (2018). MicroRNA-214-3p in the Kidney Contributes to the Development of Hypertension. J. Am. Soc. Nephrol. *29*, 2518–2528.

29. Hong, B.S., Ryu, H.S., Kim, N., Kim, J., Lee, E., Moon, H., Kim, K.H., Jin, M.S., Kwon, N.H., Kim, S., et al. (2019). Tumor Suppressor miRNA-204-5p Regulates Growth, Metastasis, and Immune Microenvironment Remodeling in Breast Cancer. Cancer Res. *79*, 1520–1534.

30. Yin, Y., Zhang, B., Wang, W., Fei, B., Quan, C., Zhang, J., Song, M., Bian, Z., Wang, Q., Ni, S., et al. (2014). miR-204-5p inhibits proliferation and invasion and enhances chemotherapeutic sensitivity of colorectal cancer cells by downregulating RAB22A. Clin. Cancer Res. *20*, 6187–6199.

31. Guo, W., Zhang, Y., Zhang, Y., Shi, Y., Xi, J., Fan, H., and Xu, S. (2015). Decreased expression of miR-204 in plasma is associated with a poor prognosis in patients with non-small cell lung cancer. Int. J. Mol. Med. *36*, 1720–1726.

32. Li, W., Jin, X., Zhang, Q., Zhang, G., Deng, X., and Ma, L. (2014). Decreased expression of miR-204 is associated with poor prognosis in patients with breast cancer. Int. J. Clin. Exp. Pathol. *7*, 3287–3292.

33. Hu, B., Sun, M., Liu, J., Hong, G., and Lin, Q. (2017). MicroRNA-204 suppressed proliferation and motility capacity of human hepatocellular carcinoma via directly targeting zinc finger E-box binding homeobox 2. Oncol. Lett. *13*, 3823–3830.

34. Ye, M., Dong, S., Hou, H., Zhang, T., and Shen, M. (2021). Oncogenic Role of Long Noncoding RNAMALAT1 in Thyroid Cancer Progression through Regulation of the miR-204/IGF2BP2/m6A-MYC Signaling. Mol. Ther. Nucleic Acids *23*, 1–12.

35. Yan, Y., Zuo, X., and Wei, D. (2015). Concise Review: Emerging Role of CD44 in Cancer Stem Cells: A Promising Biomarker and Therapeutic Target. Stem Cells Transl. Med. *4*, 1033–1043.

36. Dean, M., Fojo, T., and Bates, S. (2005). Tumour stem cells and drug resistance. Nat. Rev. Cancer *5*, 275–284.

37. Shien, K., Toyooka, S., Yamamoto, H., Soh, J., Jida, M., Thu, K.L., Hashida, S., Maki, Y., Ichihara, E., Asano, H., et al. (2013). Acquired resistance to EGFR inhibitors is associated with a manifestation of stem cell-like properties in cancer cells. Cancer Res. *73*, 3051–3061.

38. Huang, C.P., Tsai, M.F., Chang, T.H., Tang, W.C., Chen, S.Y., Lai, H.H., Lin, T.Y., Yang, J.C.H., Yang, P.C., Shih, J.Y., and Lin, S.B. (2013). ALDH-positive lung cancer stem cells confer resistance to epidermal growth factor receptor tyrosine kinase inhibitors. Cancer Lett. *328*, 144–151.

39. Alamgeer, M., Peacock, C.D., Matsui, W., Ganju, V., and Watkins, D.N. (2013). Cancer stem cells in lung cancer: Evidence and controversies. Respirology *18*, 757–764.

40. Shen, S.Q., Huang, L.S., Xiao, X.L., Zhu, X.F., Xiong, D.D., Cao, X.M., Wei, K.L., Chen, G., and Feng, Z.B. (2017). miR-204 regulates the biological behavior of breast cancer MCF-7 cells by directly targeting FOXA1. Oncol. Rep. *38*, 368–376.

41. Naor, D., Sionov, R.V., and Ish-Shalom, D. (1997). CD44: structure, function, and association with the malignant process. Adv. Cancer Res. *71*, 241–319.

42. Chen, C., Zhao, S., Karnad, A., and Freeman, J.W. (2018). The biology and role of CD44 in cancer progression: therapeutic implications. J. Hematol. Oncol. *11*, 64.

43. Suda, K., Murakami, I., Yu, H., Kim, J., Tan, A.C., Mizuuchi, H., Rozeboom, L., Ellison, K., Rivard, C.J., Mitsudomi, T., and Hirsch, F.R. (2018). CD44 Facilitates Epithelial-to-Mesenchymal Transition Phenotypic Change at Acquisition of Resistance to EGFR Kinase Inhibitors in Lung Cancer. Mol. Cancer Therapeut. *17*, 2257–2265.

44. Xu, H., Tian, Y., Yuan, X., Wu, H., Liu, Q., Pestell, R.G., and Wu, K. (2015). The role of CD44 in epithelial-mesenchymal transition and cancer development. OncoTargets Ther. *8*, 3783–3792.

45. Xu, H., Tian, Y., Yuan, X., Liu, Y., Wu, H., Liu, Q., Wu, G.S., and Wu, K. (2016). Enrichment of CD44 in basal-type breast cancer correlates with EMT, cancer stem cell gene profile, and prognosis. OncoTargets Ther. *9*, 431–444.

46. Yin, J., Zhang, H., Wu, X., Zhang, Y., Li, J., Shen, J., Zhao, Y., Xiao, Z., Lu, L., Huang, C., et al. (2020). CD44 inhibition attenuates EGFR signaling and enhances cisplatin sensitivity in human EGFR wildtype nonsmallcell lung cancer cells. Int. J. Mol. Med. *45*, 1783–1792.

47. Chang, T.H., Tsai, M.F., Su, K.Y., Wu, S.G., Huang, C.P., Yu, S.L., Yu, Y.L., Lan, C.C., Yang, C.H., Lin, S.B., et al. (2011). Slug confers resistance to the epidermal growth factor receptor tyrosine kinase inhibitor. Am. J. Respir. Crit. Care Med. *183*, 1071–1079.

48. Huang, M.H., Lee, J.H., Chang, Y.J., Tsai, H.H., Lin, Y.L., Lin, A.M.Y., and Yang, J.C.H. (2013). MEK inhibitors reverse resistance in epidermal growth factor mutation lung cancer cells with acquired resistance to gefitinib. Mol. Oncol. *7*, 112–120.

49. Liu, Y.N., Tsai, M.F., Wu, S.G., Chang, T.H., Tsai, T.H., Gow, C.H., Chang, Y.L., and Shih, J.Y. (2019). Acquired resistance to EGFR tyrosine kinase inhibitors is mediated by the reactivation of STC2/JUN/AXL signaling in lung cancer. Int. J. Cancer *145*, 1609–1624.

50. Wu, S.G., Gow, C.H., Yu, C.J., Chang, Y.L., Yang, C.H., Hsu, Y.C., Shih, J.Y., Lee, Y.C., and Yang, P.C. (2008). Frequent epidermal growth factor gene mutations in malignant pleural effusion of lung adenocarcinoma. Eur. Respir. J. *32*, 924–930.